Article

Hydrosilylation-Promoted Furan Diels–Alder Cycloadditions with Stereoselectivity Controlled by the Silyl Group

Zhi-Yun Liu, Ming Zhang, and Xiao-Chen Wang

J. Am. Chem. Soc., **Just Accepted Manuscript** • DOI: 10.1021/jacs.9b11909 • Publication Date (Web): 06 Dec 2019

Hydrosilylation-Promoted Furan Diels–Alder Cycloadditions with Stereoselectivity Controlled by the Silyl Group

Zhi-Yun Liu,† Ming Zhang,† and Xiao-Chen Wang*

State Key Laboratory and Institute of Elemento-Organic Chemistry, College of Chemistry, Nankai University, Tianjin 300071, China.

†These authors contributed equally to this work.

Correspondence: xcwang@nankai.edu.cn

ABSTRACT: Herein we describe an unprecedented $B(C_6F_5)_3$-catalyzed cascade reaction of *N*-allyl-*N*-furfurylamides involving an initial intramolecular furan Diels–Alder reaction and subsequent ether cleavage. The reaction has a broad substrate scope, even tolerating a trialkyl-substituted olefin as the dienophile, which has not previously been observed with conventional furan Diels–Alder reactions. In addition, the relative configuration of the product can be controlled by the choice of the silyl group: reactions involving Et_3SiH and $^iPr_3SiH$ gave different diastereomers. Control experiments and the computational studies revealed that the steric bulk of the silyl group plays a key role in determining the reaction pathway and thus the relative configuration of the product.

INTRODUCTION

Heterobicyclic octahydroisoindoles and analogous structural motifs are prevalent in natural products and drugs, including mitiglinide[1], serlopitant[2], and perospirone[3] (Figure 1a); and synthetic organic chemists have therefore developed efficient, selective methods for preparation

of compounds with these motifs. The existing methods include [2+2+2] cycloadditions of 1,6-enynes with alkenes[4,5] or alkynes[6,7], and cycloadditions of alkene-[8] or alkyne-tethered[9] vinylcyclopropanes, both of which are catalyzed by rhodium complexes. However, owing to the steric and electronic requirements of these metal-catalyzed cycloaddition reactions, many types of octahydroisoindoles are not accessible via these methods.

We recently became interested in an alternative approach for one-step synthesis of these structures: intramolecular furan Diels–Alder reactions of *N*-allyl-*N*-furfurylamides to afford oxygen-bridged hexahydroisoindoles (Figure 1b)[10–19]. The oxygen bridge and the olefin group of these products offer handles for further elaboration. Although this approach has been known for a long time and has been systematically studied, it remains limited in terms of substrate scope. For example, activating groups, such as halogens on the furan ring[11,15,17,18] or electron-withdrawing groups attached to the olefin[10,12,19], are often necessary for good reactivity. The cycloaddition reactions of unactivated substrates are reversible; even sterically unhindered substrates with a monosubstituted terminal olefin can undergo a retro-Diels–Alder reaction to regenerate the starting material[16]. In addition, unactivated nonterminal olefins are generally unreactive. More important, unactivated substrates lack a handle (e.g. a carbonyl group) for the association with catalysts, making external control of the stereoselectivity almost impossible, which may explain the marked decline in the number of relevant studies over the past decade. However, we have revisited this old chemistry and now report that the substrate scope can be expanded to include very sterically hindered dienophiles when the furan Diels–Alder reaction is part of a cascade process involving borane-catalyzed hydrosilylation (Figure 1c). Surprisingly, stereocontrol was also achieved, for the first time, by varying the silyl group of the hydrosilane. Experimental evidence and

computational studies suggest that the reactions proceed via two distinct mechanistic pathways, depending on the steric bulk of the silyl group.

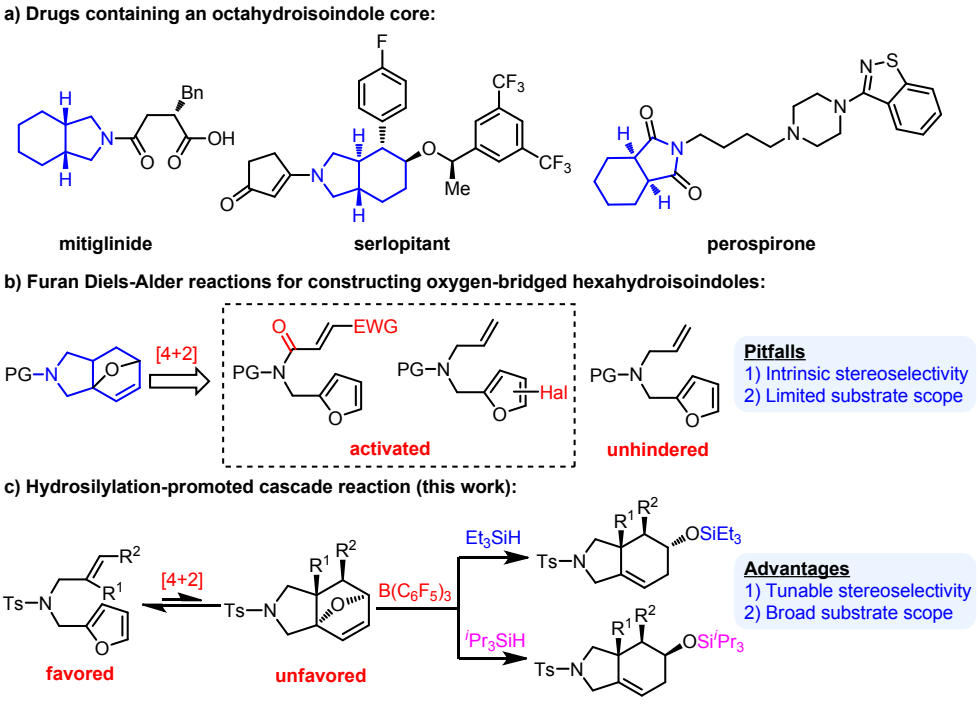

Figure 1. Syntheses and applications of hexahydroisoindoles.

RESULTS AND DISCUSSION

Our interest in borane-catalyzed hydrosilylation arose in the course of our ongoing work on the development of borane-catalyzed reactions[20–24]. Pioneering works by the groups of Piers[25–27], Oestreich[28-34], and Sakata[35] demonstrated that borane-catalyzed ketone hydrosilylation reactions proceed via activation of the hydrosilane rather than by activation of a Lewis basic carbonyl group; this activation mode is consistent with the concept of frustrated Lewis pairs introduced by Stephan and Erker[36–40]. Because of this distinct activation mechanism, borane-catalyzed hydrosilylation reactions should not be interfered with by other simultaneous reactions, as long as hydrosilane activation is not inhibited; these characteristics present opportunities for the development of new

cascade processes that take advantage of the orthogonal reactivity. We hypothesized that the above-described unfavorable [4+2] Diels–Alder cycloaddition reactions of unactivated and sterically hindered *N*-allyl-*N*-furfurylamides might become feasible if the cycloaddition product underwent a borane-catalyzed hydrosilylative ether cleavage reaction[41,42], which would drive the equilibrium of the cycloaddition reaction toward product formation.

To investigate this hypothesis, we began by carrying out reactions of furan **1a** (Table 1), whose propensity to undergo a furan Diels–Alder reaction is markedly diminished by the presence of the methyl group on the olefin. Indeed, when **1a** was heated at 120 °C in toluene for 12 h in the absence of a catalyst, Diels–Alder product **2a** was obtained in only 7% yield, with unreacted **1a** accounting for the rest of material (entry 1). However, when the reaction of **1a** was carried out in the presence of Et_3SiH and 5 mol % of $B(C_6F_5)_3$, the proposed cycloaddition/ether cleavage cascade occurred, giving hexahydroisoindole **3a** in 50% yield (entry 2), along with unidentified products generated by decomposition of the starting material. This result confirmed that the ether cleavage could shift the equilibrium of the otherwise unfavorable [4+2] cycloaddition reaction toward product formation. Other hydrosilanes (Ph_3SiH, $PhMe_2SiH$, Ph_2SiH_2, Et_2SiH_2, and $PhSiH_3$) failed to improve the yield of **3a** (entries 3–7). To our surprise, however, when we tested $^{i}Pr_3SiH$ (entry 8), we obtained not **3a** but rather **4a** (94% yield), a diastereomer with the siloxy group on the opposite face of the cyclohexene ring relative to that in **3a**, as indicated by NMR spectroscopy and single-crystal X-ray analysis.[43] Because all the stereogenic centers are formed during the furan Diels–Alder reaction, the selectivity of which is controlled solely by the electronic and steric characteristics of the substrate, we were puzzled and interested to find that the stereochemical outcome could be influenced by varying the silyl group.

Table 1. Investigation of different hydrosilanes[a]

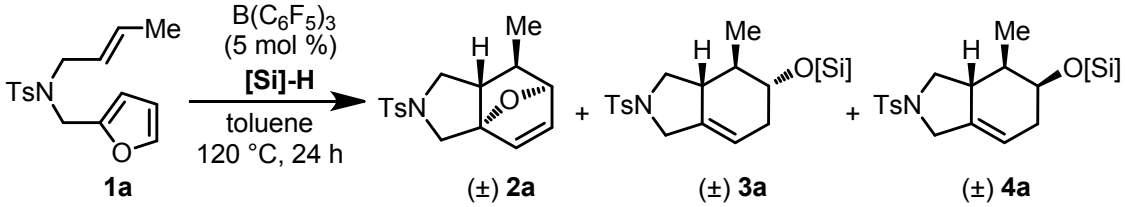

1a (±) **2a** (±) **3a** (±) **4a**

entry	[Si]-H	yield of **2a**	yield of **3a**[b]	yield of **4a**[b]
1[c]	None	7	n. d.	n. d.
2	Et_3SiH	n. d.	50	n. d.
3	Ph_3SiH	n. d.	41	n. d.
4	$PhMe_2SiH$	n. d.	26	n. d.
5	Ph_2SiH_2	n. d.	trace	n. d.
6	Et_2SiH_2	n. d.	n. d.	n. d.
7	$PhSiH_3$	n. d.	n. d.	n. d.
8[d]	$^{i}Pr_3SiH$	n. d.	trace	94

[a] The reaction was run with 0.2 mmol of **1a**, 0.3 mmol of **[Si]-H** and 5 mol % of $B(C_6F_5)_3$ in 0.5 mL of toluene in a sealed vial. [b] NMR yields determined by using CH_2Br_2 as the internal standard; n. d. = not detected. [c] No $B(C_6F_5)_3$ was added. [d] Reaction temperature: 110 °C.

Next, we investigated the generality of this silyl-group-controlled cascade process by carrying out reactions of a variety of substrates **1** in the presence of either Et_3SiH or $^{i}Pr_3SiH$ (Table 2). Reactions of **1a** with the two silanes afforded **3a** and **4a** in 45% and 85% isolated yields, respectively (entry 1). When the substituent on the *E*-olefin was changed to *n*-propyl, *i*-propyl, or benzyl (**1b**–**1d**), the cascade reaction gave exclusively or predominantly one of the two diastereomers, depending on which hydrosilane was used (entries 2–4).[43] However, reaction of substrate **1e**, which has a bromoethyl substituent, with Et_3SiH gave a complex mixture of decomposition products; whereas reaction with $^{i}Pr_3SiH$ generated **4e** in 62% yield (entry 5). Reactions with 1,1-disubstituted olefins **1f** and **1g**, which formed products with quaternary carbon centers, were also feasible (entries 6 and 7). Although the diastereoselectivities were good for

products **3f**, **3g**, and **4g**, the dr for **4f** was relatively low. The reaction of sterically unhindered substrate **1h** was highly selective with Et_3SiH but poorly selective with $^{i}Pr_3SiH$ (entry 8). Cyclizations of a substrate with a conjugated diene moiety (**1i**) occurred preferentially at the proximal olefin to give hexahydroisoindoles **3i** and **4i** (entry 9). Surprisingly, the reaction was also feasible with substrate **1j**, which has a highly hindered trisubstituted olefin, demonstrating the power of this cascade reaction (entry 10). Reactions of a series of substrates with terminal aryl groups (entries 11–16) proceeded regardless of the electronic nature of the substituents on the aromatic rings;[43] predominantly one diastereomer was obtained with both Et_3SiH and $^{i}Pr_3SiH$. Interestingly, when substrates with *Z*-olefins were tested, reactions with Et_3SiH and $^{i}Pr_3SiH$ gave the same diastereomer as the major or only product (entries 17 and 18).

Table 2. Substrate scope[a]

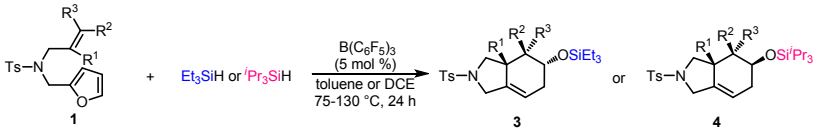

1 3 4

entry	substrate	yield of **3** (%)	yield of **4** (%)
1	**1a**	(±) **3a** 45%	(±) **4a** 85%
2	**1b**	(±) **3b** 54%	(±) **4b** 93%
3	**1c**	(±) **3c** 53%	(±) **4c** 43%
4	**1d** (*E*/*Z* = 8.5:1)	(±) **3d** 41%	(±) **4d** 84%
5	**1e**	n. d.	(±) **4e** 62%
6	**1f**	(±) **3f** 91% (dr = 8.2:1)	(±) **4f** 92% (dr = 3.3:1)
7	**1g**	(±) **3g** 64% (dr = 6.8:1)	(±) **4g** 90% (dr = 8.4:1)
8	**1h**	(±) **3h** 61% (dr = 12:1)	(±) **4h** 88% (dr = 2.4:1)
9	**1i** (E/Z = 5.1:1)	(±) **3i** 46% (*E*/*Z* = 4.5:1)	(±) **4i** 67% (E/Z = 5.5:1)
10	**1j**	(±) **3j** 54%	(±) **4j**[b] 36%
11	Ar = Ph (**1k**)	(±) **3k**, 62%	(±) **4k**, 55%
12	Ar = *p*-PhOC$_6$H$_4$ (**1l**)	(±) **3l**, 51%	(±) **4l**, 55%
13	Ar = *p*-MeC$_6$H$_4$ (**1m**)	(±) **3m**, 56%	(±) **4m**, 60%
14	Ar = *p*-FC$_6$H$_4$ (**1n**)	(±) **3n**, 67%	(±) **4n**, 69%
15	Ar = *p*-BrC$_6$H$_4$ (**1o**)	(±) **3o**, 66%	(±) **4o**, 69%
16	Ar = *p*-CF$_3$C$_6$H$_4$ (**1p**)	(±) **3p**, 62%	(±) **4p**, 59%
17	**1q**	(±) **3q** 38%	(±) **3q'** 46% (dr = 4.1:1)
18	**1r**	(±) **3r** 37%	(±) **3r'** 44% (dr = 7:1)

[a] See the supporting information for the detailed reaction conditions for each substrate. Isolated yields are given. Products having very high diastereomeric selectivity (dr > 15:1) were not labelled with the dr values. [b] 10 mol % of $B(C_6F_5)_3$ was used.

To investigate the mechanism of the reaction, and particularly the origin of the silyl-group-controlled selectivity, we conducted a number of control experiments (Figure 2). First, deuterated

hydrosilanes were subjected to reactions with **1a**. The deuterium of Et_3SiD was transferred to the allylic position of the cyclohexene (Figure 2a), indicating that addition of a hydride to the olefin unit of the Diels–Alder cycloaddition intermediate might have occurred. In contrast, the deuterium of $^{i}Pr_3SiD$ was delivered to the carbon directly connected to the siloxy group (Figure 2b), suggesting that **4a** might be the product of ketone hydrosilylation. Next, we labelled the furan with deuterium at the 5-position.[44] After reaction of deuterated **1a** with Et_3SiH, the deuterium was still at that position (Figure 2c), but when $^{i}Pr_3SiH$ was used, the deuterium shifted to the adjacent carbon (Figure 2d). These experiments indicate that the two reactions proceed via different pathways. We suspected that reactions involving Et_3SiH followed our originally intended pathway, that is, a cascade process involving a furan Diels–Alder cycloaddition and a hydrosilylative ether cleavage; whereas the reaction of $^{i}Pr_3SiH$ involved a 1,2-hydride migration and possibly a ketone hydrosilylation.

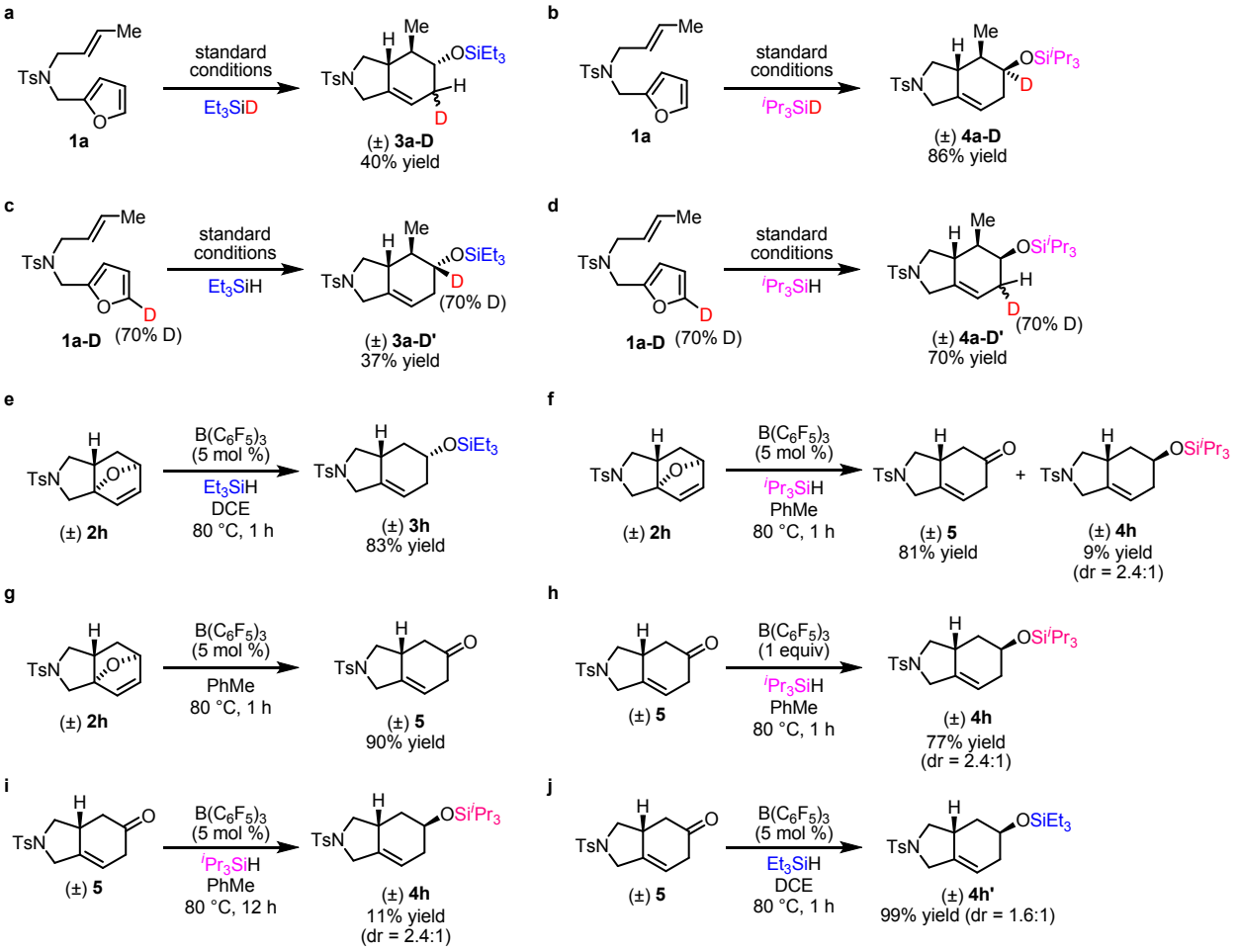

Figure 2. Mechanistic Studies

We knew that reactions of hydrosilanes with the intermediates generated by the furan Diels–Alder cycloaddition would provide more information about the overall mechanism, so we prepared cycloaddition intermediate **2h** from sterically unhindered substrate **1h**, which was the only substrate in our data table that afforded a reasonable yield of the cycloaddition intermediate under thermal conditions (see the supporting information for details). Reaction of **2h** with Et_3SiH gave corresponding cascade product **3h** in 83% yield after 1 hour at 80 °C (Figure 2e). In contrast, reaction with $^{i}Pr_3SiH$ gave only a 9% yield of **4h**, and ketone **5** was the main product (Figure 2f). Furthermore, heating **2h** with $B(C_6F_5)_3$ at 80 °C for 1 hour gave **5** in 90% yield (Figure 2g). These results provide evidence for our suspicion that the cascade reaction with $^{i}Pr_3SiH$ occurred via

ketone **5**, which was produced by means of $B(C_6F_5)_3$-promoted ring opening of **2h**. Reaction of **5** with $^{i}Pr_3SiH$ in the presence of one equivalent of $B(C_6F_5)_3$ gave **4h** in 77% yield after 1 hour (Figure 2h), and the selectivity was the same as that observed for the cascade reaction (Table 2, entry 8). However, the same reaction with only a catalytic amount of $B(C_6F_5)_3$ (5 mol %) gave a poor yield of **4h**, along with unreacted starting material (Figure 2i). These results suggest that an excess of **5** relative to the catalyst inhibited the hydrosilylation reaction, probably because **5** competed with $^{i}Pr_3SiH$ for coordination with $B(C_6F_5)_3$. Therefore, in the cascade reaction of **1h** with $^{i}Pr_3SiH$, the concentration of **5** must remain low during the reaction. In another control experiment, we found that reaction of **5** with Et_3SiH gave a mixture of diastereomers with a poor dr (Figure 2j). Considering that the cascade reaction of **1h** with Et_3SiH showed excellent diastereoselectivity (Table 2, entry 8), we concluded that the cascade reaction with Et_3SiH proceeded exclusively via hydrosilylative cleavage of the oxygen bridge, rather than via hydrosilylation of a ketone intermediate.

On the basis of the above-described experimental results, we propose the reaction mechanisms shown in Figure 3. In the cascade reaction of **1a** with Et_3SiH (Figure 3a), cycloaddition intermediate **2a** reacts with borane-activated hydrosilane complex **6** to give ion pair **7**, in which the silylium ion is bound to the oxygen bridge. Ring opening and subsequent delivery of hydride to the allylic carbocation of **8** gives product **3a** and regenerates the catalyst. The calculated free energy profile of this process is shown in Figure 3b. The intramolecular furan Diels–Alder reaction to afford **2a** is endothermic by 1.2 kcal/mol and has an energy barrier of 28.8 kcal/mol (**TS1**), which is qualitatively in agreement with our experimental observation that the equilibrium favors the starting material (**1a**). In addition, *exo* cycloaddition (**TS1**) is strongly favored over *endo* cycloaddition (**TS1'**, 39.0 kcal/mol), and therefore a single isomer forms during

the cycloaddition. Subsequent hydrosilylative ether cleavage (conversion of **2a** to **3a**) has an overall barrier of 12.4 kcal/mol (from **2a** to **TS3**), which is much lower than the barrier of the furan Diels–Alder reaction, indicating that the cycloaddition reaction is rate-limiting. Furthermore, the final step of the process, hydride addition to the allylic carbocation of **8** to form **3a** is barrier-less and is very exothermic (−44.3 kcal/mol).

The proposed mechanism for the reaction with $^{i}Pr_3SiH$ involves two co-existing catalytic cycles (**A** and **B** in Figure 3c). In the cycle **A**, $B(C_6F_5)_3$ binds to the oxygen bridge of **2a** to form complex **9**, which undergoes ring opening to give zwitterionic intermediate **10**. Then a 1,2-hydride shift gives borane-ketone complex **11**. Dissociation of $B(C_6F_5)_3$ from **11** generates ketone **12**, which enters catalytic cycle **B**, the borane-catalyzed ketone hydrosilylation reaction. In this cycle, hydride is transferred from $HB(C_6F_5)_3^-$ to the silyl-activated carbonyl group of bicyclic species **14** from the less-hindered face (opposite the methyl group), which results in the observed stereochemical features of **4a**. The free energy profile of the overall process is shown in Figure 3d. Owing to the steric bulk of the silyl group, the mechanism depicted in Figure 3a becomes energetically unfavorable (from **2a** to **TS9**, 27.4 kcal/mol). Instead, from **2a**, $B(C_6F_5)_3$-mediated ring opening with 1,2-hydride migration to form borane-ketone complex **11**, which is exothermic (−27.4 kcal/mol) and has a barrier of 13.2 kcal/mol, is the predominant reaction pathway. The subsequent ketone hydrosilylation reaction has a barrier of 24.7 kcal/mol (from **11** to **TS7**). The addition of hydride to the silyl-activated carbonyl group from the less-hindered face is favored by 3.5 kcal/mol (**TS8** vs. **TS10**), in agreement with the excellent diastereocontrol observed in the reaction of **1a** with $^{i}Pr_3SiH$. The furan Diels–Alder reaction is again the rate-determining step for the overall process, and therefore the concentration of ketone intermediate **12** should be low because the ketone is readily converted to the final product. In fact, the experiment shown in Figure

2i indicates that the low ketone concentration is essential to prevent catalyst inhibition by excess ketone.

Notably, the Gibbs free energies shown in Figure 3b and Figure 3d were calculated at 120 °C (393 K) and 110 °C (383 K), respectively, in accordance with the respective optimal reaction temperature. We have also calculated the pathway shown in Figure 3d when Et_3SiH was applied in place of $^{i}Pr_3SiH$ at 120 °C (393 K). The obtained free energy profile is given in the supporting information as Figure S1. The energy profile indicates that this pathway is less favorable than the pathway depicted in Figure 3b because of the relatively high energy of **TS5** (14.9 kcal/mol at 120 °C) compared to **TS3** in Figure 3b (13.6 kcal/mol), which is qualitatively in agreement with the experimental result.

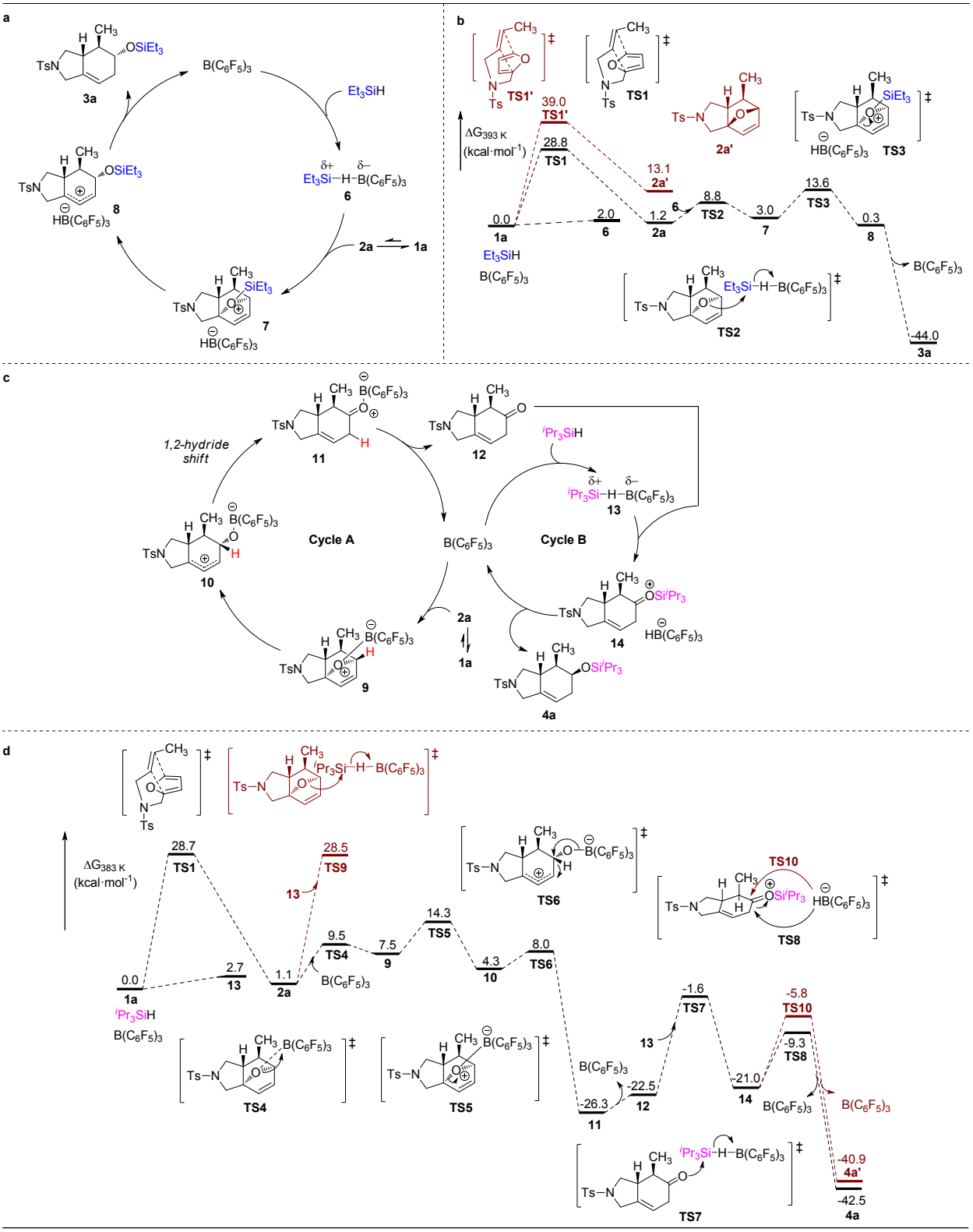

Figure 3. a, Proposed mechanism of the reaction of **1a** with Et_3SiH. **b**, Energy profile of the reaction with Et_3SiH at 393 K. **c**, Proposed mechanism of the reaction of **1a** with $^{i}Pr_3SiH$. **d**, Energy

profile of the reaction with $^{i}Pr_3SiH$ at 383 K. DFT calculations were performed using M06-2X-D3/6-311++G(d,p)/SMD(toluene)//M06-2X/6-31G(d).

We then explored the synthetic utility of this methodology by carrying out some transformations of **4a** (Figure 4). The tosyl protecting group could easily be removed by reaction with magnesium to afford free amine **15**. In addition, the olefin could be transformed either to epoxides (***trans*-16** and ***cis*-16**) via oxidation with *m*-CPBA or to hydroxyl compounds (***cis*-17** and ***trans*-17**) via hydroboration followed by oxidation. Furthermore, the silyl group could be cleaved with TBAF to give unprotected hydroxyl compound **18**, which could be oxidized with PCC to give ketone **12**[45] or hydrogenation over Pd/C to give *cis*-bicyclic octahydroisoindole **19**, in excellent yields in both cases.

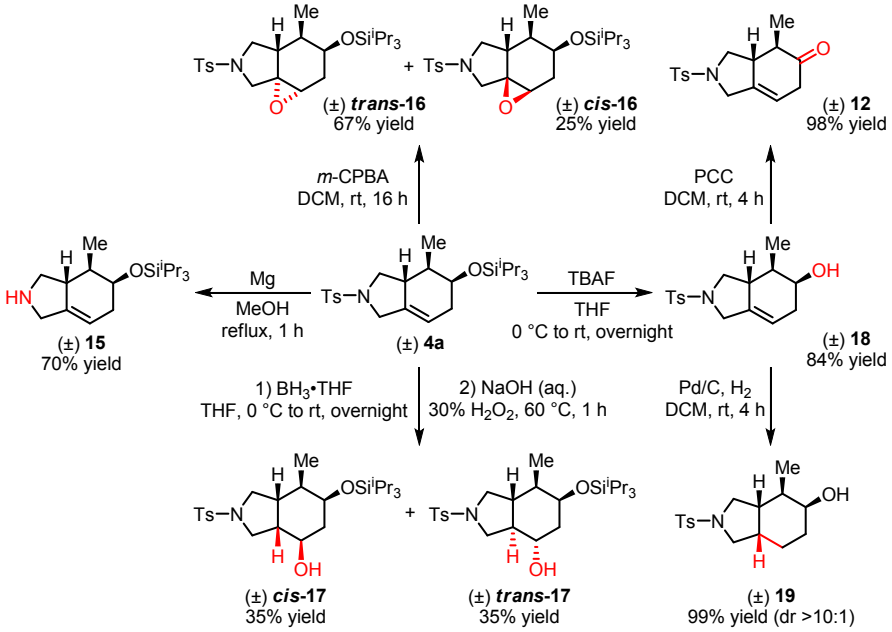

Figure 4. Transformations of 4a

CONCLUSIONS

In summary, we overcame the narrow substrate scope of intramolecular furan Diels–Alder reactions of *N*-allyl-*N*-furfurylamides by developing a cascade process that involves a borane-

catalyzed hydrosilylation reaction. Furthermore, the stereoselectivity was controlled by the hydrosilane. Control experiments and computational studies were performed to elucidate the mechanism of the reactions, which involve either hydrosilylative ether cleavage or borane-catalyzed ether cleavage followed by ketone hydrosilylation, depending on the hydrosilane that is used. Furthermore, the reaction generates structurally interesting and synthetically useful heterobicyclic compounds, which are not readily accessible by other methods. The chemistry showcases the power of borane-catalyzed hydrosilylation reactions. Our results can be expected to lead to the development of additional cascade processes involving borane-catalyzed hydrosilylation.

ASSOCIATED CONTENT

Supporting Information. Experimental details, compound characterization data, spectra (PDF), and X-ray diffraction data (CIF). This material is available free of charge via the Internet at http://pubs.acs.org.

AUTHOR INFORMATION

Corresponding Author

*xcwang@nankai.edu.cn

ORCID

Xiao-Chen Wang: 0000-0001-5863-0804

Notes

The authors declare no competing financial interests.

Author Contributions

Z.-Y.L. and M.Z. contributed equally to this work.

ACKNOWLEDGMENT

We thank financial support from the National Natural Science Foundation of China (91956106 and 21871147), and the Fundamental Research Funds for Central Universities. We thank Prof. Xiufang Xu, Prof. Shou-Fei Zhu and Prof. Qian Peng for assistance with DFT calculations.

REFERENCES

1. Sunaga, Y.; Gonoi, T.; Shibasaki, T.; Ichikawa, K.; Kusama, H.; Yano, H.; Seino, S. The effects of mitiglinide (KAD-1229), a new anti-diabetic drug, on ATP-sensitive K^+ channels and insulin secretion: comparison with the sulfonylureas and nateglinide. *Eur. J. Pharmacol.* **2001**, *431*, 119–125.

2. Yosipovitch, G.; Stander, S.; Kerby, M. B.; Larrick, J. W.; Perlman, A. J.; Schnipper, E. F.; Zhang, X.; Tang, J. Y.; Luger, T.; Steinhoff, M. Serlopitant for the treatment of chronic pruritus: results of a randomized, multicenter, placebo-controlled phase 2 clinical trial. *J. Am. Acad. Dermatol.* **2018**, *78*, 882–891.e10.

3. Onrust, S. V.; McClellan, K. Perospirone. *CNS Drugs* **2001**, *15*, 329–337.

4. Masutomi, K.; Sakiyama, N.; Noguchi, K.; Tanaka, K. Rhodium-catalyzed regio-, diastereo-, and enantioselective [2+2+2] cycloaddition of 1,6-enynes with acrylamides. *Angew. Chem., Int. Ed.* **2012**, *51*, 13031–13035.

5. Masutomi, K.; Sugiyama, H.; Uekusa, H.; Shibata, Y.; Tanaka, K. Asymmetric synthesis of protected cyclohexenylamines and cyclohexenols by rhodium-catalyzed [2+2+2] cycloaddition. *Angew. Chem., Int. Ed.* **2016**, *55*, 15373–15376.

6. Evans, P. A.; Lai, K. W.; Sawyer, J. R. Regio- and enantioselective intermolecular rhodium-catalyzed [2+2+2] carbocyclization reactions of 1,6-enynes with methyl arylpropiolates. *J. Am. Chem. Soc.* **2005**, *127*, 12466–12467.

7. Shibata, T.; Arai, Y.; Tahara, Y. Enantioselective construction of quaternary carbon centers by catalytic [2 + 2 + 2] cycloaddition of 1,6-enynes and alkynes. *Org. Lett.* **2005**, *7*, 4955–4957.

8. Wender, P. A.; Haustedt, L. O.; Lim, J.; Love, J. A.; Williams, T. J.; Yoon, J.-Y. Asymmetric catalysis of the [5 + 2] cycloaddition reaction of vinylcyclopropanes and π-systems. *J. Am. Chem. Soc.* **2006**, *128*, 6302–6303.

9. Jiao, L.; Lin, M.; Zhuo, L.-G.; Yu, Z.-X. Rh(I)-catalyzed [(3 + 2) + 1] cycloaddition of 1-yne/ene-vinylcyclopropanes and CO: homologous Pauson-Khand reaction and total synthesis of (±)-α-agarofuran. *Org. Lett.* **2010**, *12*, 2528–2531.

10. Isaacs, N. S.; Van der Beeke, P. Reactions at high pressure, part 10: The volume profile of an intramolecular Diels-Alder Reaction. *Tetrahedron Lett.* **1982**, *23*, 2147–2148.

11. Klepo, Z.; Jakopcic, K. Studies in the furan series. 23. Preparation of some new 5-substituted furfurylallylarylamines. Influence of substituents on the intramolecular Diels-Alder (IMDA) reaction. *J. Heterocycl. Chem.* **1987**, *24*, 1787–1791.

12. Jung, M. E.; Gervay, J. Solvent effects in intramolecular Diels-Alder reactions of 2-furfuryl methyl fumarates: Evidence for a polar transition state. *J. Am. Chem. Soc.* **1989**, *111*, 5469–5470.

13. Kappe, C. O.; Murphree, S. S.; Padwa, A. Synthetic applications of furan Diels-Alder chemistry. *Tetrahedron* **1997**, *53*, 14179–14233.

14. Ghelfi, F.; Parsons, A. F.; Tommasini, D.; Mucci, A. Intramolecular Diels-Alder cycloaddition of *N*-allyl-*N*-(2-furylmethyl)amides – First step of a new route towards the synthesis of a densely functionalized pyrrolizidine ring. *Eur. J. Org. Chem.* **2001**, 1845–1852.

15. Crawford, K. R.; Bur, S. K.; Straub, C. S.; Padwa, A. Intramolecular cyclization reactions of 5-halo- and 5-nitro-substituted furans. *Org. Lett.* **2003**, ***5***, 3337–3340.

16. Kuhnert, N.; Sammes, P. G.; Smith G.; Ward, R. W. A powerful aqueous solvent effect in an intramolecular Diels–Alder cyclisation. *J. Chem. Res.* **2004**, 608–610.

17. Pieniazek, S. N.; Houk, K. N. The origin of the halogen effect on reactivity and reversibility of Diels–Alder cycloadditions involving furan. *Angew. Chem., Int. Ed.* **2006**, *45*, 1442–1445.

18. Padwa, A.; Crawford, K. R.; Straub, C. S.; Pieniazek, S. N.; Houk, K. N. Halo substituent effects on intramolecular cycloadditions involving furanyl amides. *J. Org. Chem.* **2006**, *71*, 5432–5439.

19. Yamazaki, S.; Sugiura, H.; Niina, M.; Mikata, Y.; Ogawa, A. Inter- and Intramolecular Diels-Alder reaction of ethenetricarboxylate derivatives. *Heterocycles* **2016**, *92*, 485–510.

20. Zhang, Z.-Y.; Liu, Z.-Y.; Guo, R.-T.; Zhao, Y.-Q.; Li, X.; Wang, X.-C. $B(C_6F_5)_3$-catalyzed ring opening and isomerization of unactivated cyclopropanes. *Angew. Chem., Int. Ed.* **2017**, *56*, 4028–4032.

21. Liu, Z.-Y.; Wen, Z.-H.; Wang, X.-C. $B(C_6F_5)_3$-catalyzed cascade reduction of pyridines. *Angew. Chem., Int. Ed.* **2017**, *56*, 5817–5820.

22. Tu, X.-S.; Zeng, N.-N.; Li, R.-Y.; Zhao, Y.-Q.; Xie, D.-Z.; Peng, Q.; Wang, X.-C. C_2-symmetric bicyclic bisborane catalysts: kinetic or thermodynamic products of a reversible hydroboration of dienes. *Angew. Chem., Int. Ed.* **2018**, *57*, 15096–15100.

23. Tian, J.-J.; Zeng, N.-N.; Liu, N.; Tu, X.-S.; Wang, X.-C. Intramolecular cyclizations of vinyl-substituted *N*,*N*-dialkyl arylamines enabled by borane-assisted hydride transfer. *ACS Catal.* **2019**, *9*, 295–300.

24. Li, X.; Tian, J.-J.; Liu, N.; Tu, X.-S.; Zeng, N.-N.; Wang, X.-C. Spiro-bicyclic bisborane catalysts for metal-free chemoselective and enantioselective hydrogenation of quinolines. *Angew. Chem., Int. Ed.* **2019**, *58*, 4664–4668.

25. Parks, D. J.; Piers, W. E. Tris(pentafluorophenyl)boron-catalyzed hydrosilation of aromatic aldehydes, ketones, and esters. *J. Am. Chem. Soc.* **1996**, *118*, 9440–9441.

26. Parks, D. J.; Blackwell, J. M.; Piers, W. E. Studies on the mechanism of $B(C_6F_5)_3$-catalyzed hydrosilation of carbonyl functions. *J. Org. Chem.* **2000**, *65*, 3090–3098.

27. Houghton, A. Y.; Hurmalainen, J.; Mansikkamäki, A.; Piers, W. E.; Tuononen, H. M. Direct observation of a borane–silane complex involved in frustrated Lewis-pair-mediated hydrosilylations. *Nat. Chem.* **2014**, *6*, 983–988.

28. Rendler, S.; Oestreich, M. Conclusive Evidence for an S_N2-Si Mechanism in the $B(C_6F_5)_3$-catalyzed hydrosilylation of carbonyl compounds: Implications for the related hydrogenation. *Angew. Chem. Int. Ed.* **2008**, *47*, 5997–6000.

29. Hermeke, J.; Mewald, M.; Oestreich, M. Experimental analysis of the catalytic cycle of the borane-promoted imine reduction with hydrosilanes: spectroscopic detection of unexpected intermediates and a refined mechanism. *J. Am. Chem. Soc.* **2013**, *135*, 17537−17546.

30. Simonneau, A.; Oestreich, M. 3-Silylated Cyclohexa-1,4-dienes as precursors for gaseous hydrosilanes: the $B(C_6F_5)_3$-catalyzed transfer hydrosilylation of alkenes. *Angew. Chem. Int. Ed.* **2013**, *52*, 11905–11907.

31. Oestreich, M.; Hermeke, J.; Mohr, J. A unified survey of Si–H and H–H bond activation catalysed by electron-deficient boranes. *Chem. Soc. Rev.* **2015**, *44*, 2202–2220.

32. Simonneau, A.; Oestreich, M. Formal SiH_4 chemistry using stable and easy-to-handle surrogates. *Nat. Chem.* **2015**, *7*, 816–822.

33. Yuan, W.; Smirnov, P.; Oestreich, M. Custom hydrosilane synthesis based on monosilane. *Chem* **2018**, *4*, 1443–1450.

34. Wu, Q.; Irran, E.; Müller, R.; Kaupp, M.; Klare, H. F. T.; Oestreich, M. Characterization of hydrogen-substituted silylium ions in the condensed phase. *Science* **2019**, *365*, 168–172.

35. Sakata, K.; Fujimoto, H. Quantum chemical study of $B(C_6F_5)_3$−catalyzed hydrosilylation of carbonyl group. *J. Org. Chem.* **2013**, *78*, 12505–12512.

36. Stephan, D. W.; Erker, G. Frustrated Lewis pair chemistry: Development and perspectives. *Angew. Chem., Int. Ed.* **2015**, *54*, 6400–6441.

37. Stephan, D. W. Frustrated Lewis pairs: From concept to catalysis. *Acc. Chem. Res.* **2015**, *48*, 306−316.

38. Stephan, D. W. The broadening reach of frustrated Lewis pair chemistry. *Science* **2016**, *354*, aaf7229-1− aaf7229-8.

39. Lam, J.; Szkop, K. M.; Mosaferi, E.; Stephan, D. W. FLP catalysis: main group hydrogenations of organic unsaturated substrates. *Chem. Soc. Rev.* **2019**, *48*, 3592–3612.

40. Stephan, D. W. Frustrated Lewis pairs. *J. Am. Chem. Soc.* **2015**, *137*, 10018−10032.

41. Gevorgyan, V.; Liu, J.-X.; Rubin, M.; Benson, S.; Yamamoto, Y. A novel reduction of alcohols and ethers with a $HSiEt_3$/catalytic $B(C_6F_5)_3$ system. *Tetrahedron Lett.* **1999**, *40*, 8919–8922.

42. Gevorgyan, V.; Rubin, M.; Benson, S.; Liu, J.-X.; Yamamoto, Y. A Novel $B(C_6F_5)_3$-catalyzed reduction of alcohols and cleavage of aryl and alkyl ethers with hydrosilanes. *J. Org. Chem.* **2000**, *65*, 6179–6186.

43. CCDC 1957769 (**4a**), 1957770 (**3b**), 1957771 (**3k**) and 1957774 (**4n**) contain the supplementary crystallographic data for this paper. These data are provided free of charge by The Cambridge Crystallographic Data Centre.

44. We were unable to achieve higher than 70% of the deuterium incorporation at the 5-position.

45. Indeed, ketone **12** could be alternatively obtained by reacting **1a** in toluene at 110 °C for 24 h in the presence of 5 mol % of $B(C_6F_5)_3$ without the addition of any hydrosilanes. However, the NMR yield of **12** was merely 22% because of the severe decomposition of **1a** under these conditions.

TOC

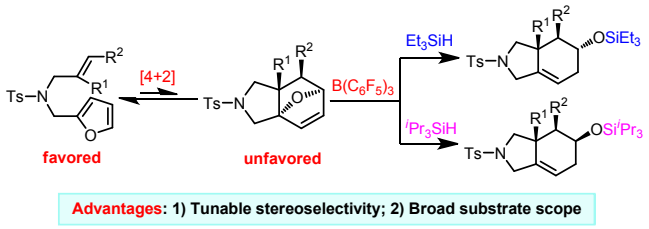

Advantages: 1) Tunable stereoselectivity; 2) Broad substrate scope